Ten Years of Measurements of Tropical Upper-Tropospheric Water Vapor by MOZAIC. Part I: Climatology, Variability, Transport, and Relation to Deep Convection

ZHENGZHAO LUO, DIETER KLEY,* AND RICHARD H. JOHNSON

Department of Atmospheric Science, Colorado State University, Fort Collins, Colorado

HERMAN SMIT

Institute for Chemistry and Dynamics of the Geosphere: Troposphere (ICG-II), Research Centre Juelich GmbH, Juelich, Germany

(Manuscript received 6 February 2006, in final form 3 May 2006)

ABSTRACT

Ten years (1994–2004) of measurements of tropical upper-tropospheric water vapor (UTWV) by the Measurement of Ozone and Water Vapor by Airbus In-Service Aircraft (MOZAIC) are investigated over three regions—the tropical Atlantic, tropical Africa, and the Asian monsoon region—to determine the UTWV climatology and variability on multiple scales and to understand them in relation to moisture transport and deep convection.

The seasonal migration of upper-tropospheric humidity (UTH) keeps pace with that of the ITCZ, indicating the convective influence on UTH distribution. Some significant regional differences are identified with the tropical Africa and the Asian monsoon regions being moister than the tropical Atlantic. UTH generally increases with height by 10%–20% relative humidity with respect to ice (RHi) from about 300 to 200 hPa, and the differences are larger in the deep Tropics than in the subtropics. The probability density functions of tropical UTH are often bimodal. The two modes stay rather constant; differences in the mean value are largely due to the variations in the proportion of the two modes as opposed to changes in the modes themselves. In the deep Tropics, the moisture level frequently reaches ice supersaturation, the most notable case being the near-equatorial Asian monsoon region during the wet season when ice supersaturation is observed 46% of the time.

Interannual variations are observed in association with the 1997–98 ENSO event. A warming of about 1–2 K is observed for all three regions equatorward of roughly 15°. Specific humidity also increases somewhat for the tropical Atlantic and tropical Africa, but the increase in temperature outweighs the increase in specific humidity such that RH decreases by 5%–15% RHi. In addition to the ENSO-related variation, MOZAIC also sees increases in both RH and specific humidity over tropical Africa from 2000 onward.

Moisture fluxes are computed from MOZAIC data and decomposed into contributions from the mean circulation and from eddies. The flux divergence, which represents the moisture source/sink from horizontal transport, is also estimated. Finally, the MOZAIC climatology and variability are revisited in relation to deep convection obtained from the International Satellite Cloud Climatology Project (ISCCP).

1. Introduction

Water vapor is the key atmospheric constituent for the earth's hydrological cycle and the most important greenhouse gas in the climate system. It is highly variable on multiple spatial and temporal scales and is usually expected to be increasing under a global warming scenario resulting in an amplification of the CO_2 greenhouse effect (e.g., Cess et al. 1990). Unfortunately, water vapor in the atmosphere is not measured with a high degree of accuracy (compared to the measurements of temperature and pressure, e.g.), neither by the global radiosonde network nor by satellites. The difficulties are particularly compounded in the upper troposphere, where radiosonde humidity sensors fail at low temperature (Elliot and Gaffen 1991; Wang et al. 2003) and satellite sensors provide only coarse vertical and hori-

* Additional affiliation: Institute for Chemistry and Dynamics of the Geosphere: Troposphere (ICG-II), Research Centre Juelich GmbH, Juelich, Germany.

Corresponding author address: Dr. Zhengzhao Luo, Department of Atmospheric Science, Colorado State University, Fort Collins, CO 80523.
E-mail: luo@atmos.colostate.edu

zontal resolutions (Soden and Bretherton 1993; Stephens et al. 1996). Moreover, high cloudiness often prevents accurate retrieval of upper-tropospheric water vapor (UTWV) information from satellites (Wu et al. 1993; Bates et al. 1996). Consequently, our understanding of the processes that control UTWV is far from complete. An illuminating example is the debate initiated by Lindzen (1990) over the role of UTWV in climate change, in which he speculated a potential drying of the tropical upper troposphere during global warming. Although existing evidence leans against such a controversial view (Held and Soden 2000; Pierrehumbert et al. 2007), the debate itself highlights the need for more studies of UTWV and related processes.

In addition to radiosondes and satellites, aircraft is another source of UTWV data. The Measurement of the Ozone and Water Vapor by Airbus In-Service Aircraft (MOZAIC) project funded by the European Union features more than 10 yr of continuous measurements of water vapor and ozone (along with position, pressure, temperature, and winds) around the globe (with the exception of the Pacific and Australia) starting from August 1994. The MOZAIC data on upper-tropospheric humidity (UTH) have a quality-assured mean accuracy of 5% (Helten et al. 1998, 1999), which is superior to that of most other humidity data sources. UTH data with high vertical resolution, more accurate than those from MOZAIC, are only obtainable from campaign-style research instrumentation on dedicated balloons and research aircraft (Kley et al. 2000). Most of the previous studies using the MOZAIC data addressed the ozone-related atmospheric chemistry topics (e.g., Thouret et al. 1998). A handful of research has been directed toward the study of UTWV in specific areas such as ice supersaturation (Gierens and Spichtinger 2000) and UTH distribution law (Gierens et al. 1999). None of these works, however, has examined from a global perspective the UTWV climatology and variability. The 10-yr period of MOZAIC data is long enough to compile a reliable climatology and capture a couple of ENSO cycles.

In this study, an important first step is undertaken to fill a gap in the utilization of the MOZAIC data by documenting the UTVW temporal and spatial distribution and variability from seasonal to interannual time scales. There have been very few, if any, high-quality, long-term, near-global in situ measurements of UTWV due to a variety of observational difficulties. MOZAIC data provide an opportunity to correct this situation. However, in addition, we place these observations in the context of our understanding of climate dynamics of the upper troposphere. While some of the results confirm the well-known features of the UTWV climatology obtained from radiosondes and satellite observations, many others are unique and can only be found by MOZAIC (e.g., the frequent observation of ice supersaturation). Only the Tropics (30°S–30°N)[1] are considered because the flight levels of the MOZAIC aircraft (about 300–200 hPa) are almost always below the tropical tropopause layer (TTL) there, but may extend into the lower stratosphere in midlatitudes. The uniqueness of the MOZAIC data also makes them a valuable source for evaluating other UTWV products, especially those from reanalyses. UTH distributions in reanalyses data are sensitive to the convection and cloud parameterizations used in the data assimilation system, just like in any general circulation and climate models (e.g., Pope et al. 2001). Such a comparison study will be carried out in a companion paper (Z. Luo et al. 2006, unpublished manuscript).

Another aspect of this paper is a study of the influence on the UTWV distribution of moisture transport and deep convection. Since both relative humidity (RH) and flight-level winds $\mathbf{v}$ are measured directly by the MOZAIC aircraft and simultaneous measurements of temperature allow computation of specific humidity (q), moisture flux $\mathbf{v}q$ at flight level can be calculated. Previous studies of the effect of large-scale advection usually rely on the wind fields from reanalyses (e.g., Pierrehumbert and Rocca 1998). Unlike midlatitudes, however, there are very few observations in the Tropics to feed the data assimilation system, and there are also very few dynamical constraints in low latitudes (such as the quasigeostrophic approximation). Therefore, the 3D circulation from reanalyses is considered less reliable in the Tropics. Although MOZAIC data are generally confined to several levels in the upper troposphere, 10 yr of MOZAIC-based moisture fluxes are an alternative (and more accurate) data source for studying tropical UTWV transports and their influence on the UTWV distribution.

Deep convection is another important player that affects the tropical UTWV distribution in a profound way (Soden and Fu 1995; Udelhofen and Hartmann 1995; Salathe and Hartmann 1997; Soden 2004; Luo and Rossow 2004). As will be shown in this paper, many specific features of the MOZAIC climatology and variability cannot be fully understood without analyzing a collocated deep convection dataset. The International Satellite Cloud Climatology Project (ISCCP), which has produced a 21-yr-long (from August 1983 to December

[1] We follow this definition of the Tropics throughout this paper; it actually includes both the deep Tropics and subtropics.

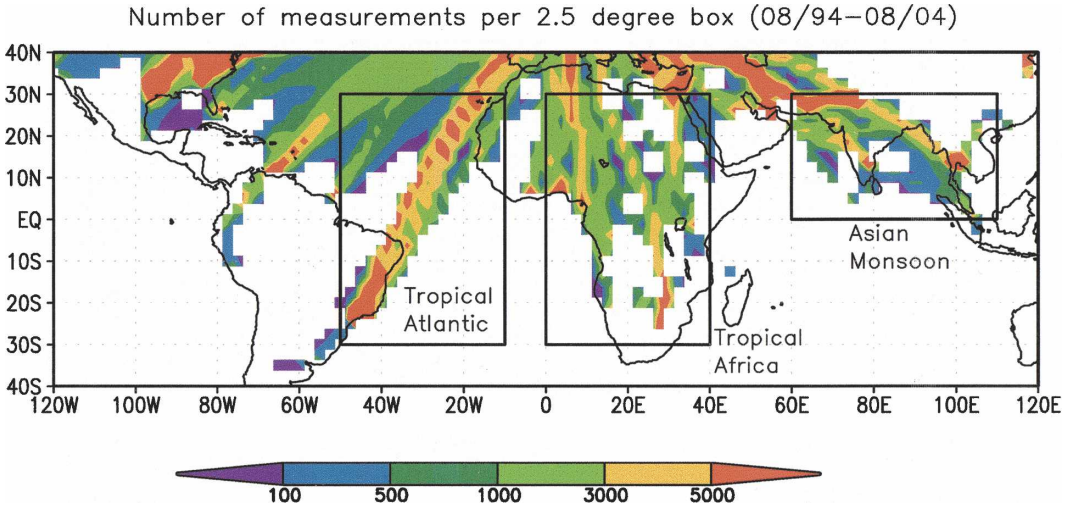

FIG. 1. Geographical map of the three tropical regions and the flight density.

2004), 3-hourly–30-km cloud climatology (Rossow and Schiffer 1999), is used in this study to identify deep convection.

Three tropical regions are selected for detailed analysis owing to their climatological importance and the geographical coverage of the MOZAIC flights (Fig. 1): the tropical Atlantic (30°S–30°N, 50°–10°W), tropical Africa (30°S–30°N, 0°–40°E), and the Asian monsoon region (0°–30°N, 60°–110°E). The lack of MOZAIC data south of the equator in the Asian monsoon sector restricts our analysis of this region to the Northern Hemisphere. The paper is organized as follows: The MOZAIC project and dataset are described in section 2. In section 3, we document and discuss several aspects of the MOZAIC climatology including UTH annual cycle, vertical structure, and probability density function. Section 4 examines the UTH interannual variability. Section 5 focuses on moisture fluxes and transport. In section 6, the ISCCP deep convection data are utilized to reexamine the MOZAIC climatology and variability. Finally, a summary and conclusions are given in section 7.

2. MOZAIC program and data

MOZAIC is a project, funded by the European Union, for the measurement of the large-scale distribution of ozone and water vapor onboard commercial Airbus A340 aircraft during scheduled flights (Marenco et al. 1998). Five A340 long-range passenger aircraft are equipped with semiautomated instrumentation to measure relative humidity, ozone, and temperature and to record aircraft data such as position, pressure, temperature, wind speed, Mach number, etc. MOZAIC equipment is flown during scheduled flights by several European airlines. MOZAIC was launched in January 1993 and has been operational since August 1994. It was originally funded for three years, not long enough to generate meaningful climatology or to analyze for long-term variability of UTH. Fortunately, the project's lifetime was extended several times. At present, MOZAIC is still ongoing and data exist since its inception in August 1994. More than 2500 flights/year with a total of about 125 000 flight hours of measurements were made as of December 2003. The flights cover all continents, except Australia, and all oceans except the Pacific. Roughly 32% of the flights cover the three tropical regions that are selected for detailed analysis: tropical Africa, Asian monsoon region, and tropical Atlantic (Fig. 1). The time resolution of the MOZAIC humidity measurements in the upper troposphere is 1 min, which, at cruising speed, corresponds to a spatial resolution of 15 km. In the tropical regions, MOZAIC aircraft at cruise altitude fly at five discrete pressure levels of 288, 262, 238, 217, and 197 hPa, which are almost always below the TTL.

It is probably helpful to clarify the meaning of some terms used in this paper: we use UTH to mean the upper-tropospheric relative humidity (RH), whereas UTWV is used to indicate the upper-tropospheric moisture in general. RHi refers to relative humidity with respect to ice. UTH is often used by the satellite community to refer to the average RH over a thick layer between roughly 500 and 200 mb as measured by the satellite water vapor channel (~6.7 μm). In this study, the MOZAIC-based UTH does not have any satellite linkage, but denotes the in situ measurements of RH at the aircraft flight level.

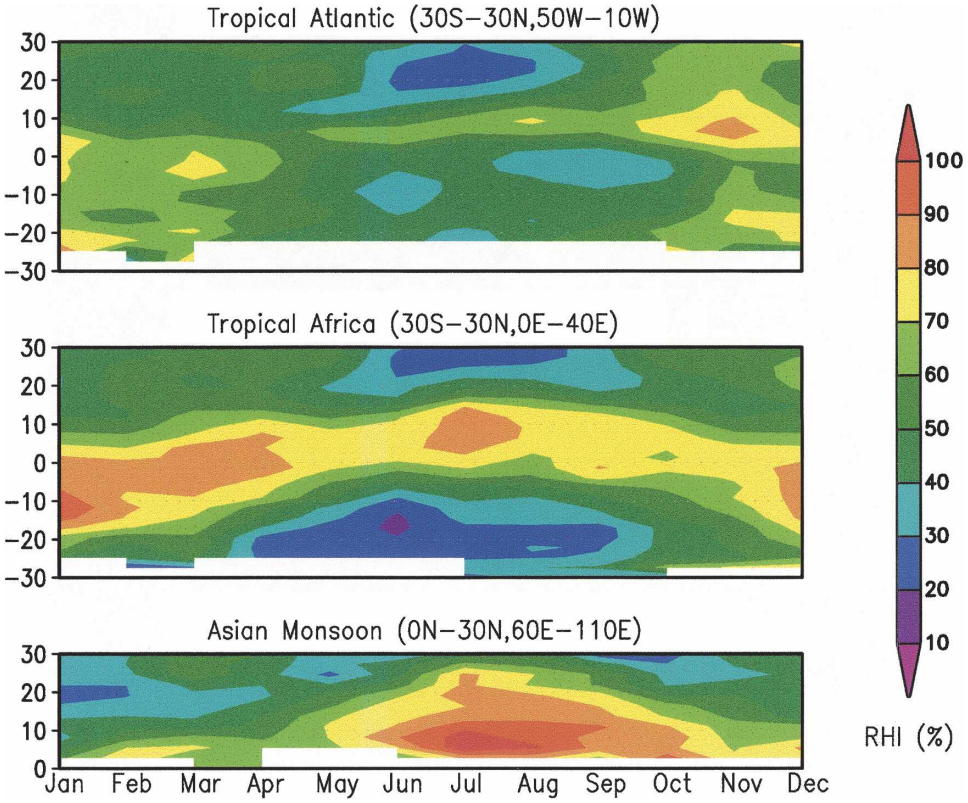

FIG. 2. Composite annual cycle of UTH or RHi as a function of latitude.

3. MOZAIC climatology

Nawrath (2002) analyzed four years (1996–2000) of MOZAIC climatology for the flights between Europe and South America covering the tropical Atlantic region. In this section, we expand her work by including more regions (tropical Africa and Asian monsoon region) and covering a longer period of time (August 1994–April 2004). We also augment her climatology by constructing the composite annual cycle of UTH. The following three aspects of the UTH climatology are examined: annual cycle, vertical structure, and probability density function. The regional differences are also identified and discussed.

a. Annual cycle

Based on nearly 10 yr of data, we construct a composite annual cycle of UTH for the three tropical regions. Figure 2 shows the UTH annual cycle (with respect to ice, i.e., RHi) as a function of latitude. All levels are included (the difference in RHi between different MOZAIC flight levels is usually 10%–20% RHi; see section 3b). In general, the seasonal migration of the UTH pattern keeps pace with that of the ITCZ in the corresponding region (Waliser and Gautier 1993), indicating the convective influence on the UTH distribution. The effect of convection on UTH will be better recognized in section 6 where we explicitly study the relationship between UTH and convection using both MOZAIC and ISCCP data. Some significant regional differences are identified in Fig. 2: 1) the magnitude of the UTH seasonal cycle is large for the South Asian monsoon region and tropical Africa and it is comparatively weak for the tropical Atlantic; 2) the moistest upper troposphere is found in the Asian monsoon region during the wet season (with the monthly mean RHi greater than ice saturation), followed by tropical Africa during the local summer, while it is least likely to see a very moist upper troposphere in the tropical Atlantic; and 3) subtropical Africa south of the equator (10°–30°S) experiences the driest upper troposphere for the most prolonged period during the local winter (i.e., boreal summer) with values of RHi only around 20%[2] and is much drier than the Sahara desert region. These regional differences can be explained by the dif-

[2] Note that this number will become even smaller if considered with respect to water, as in most satellite-based UTH retrievals.

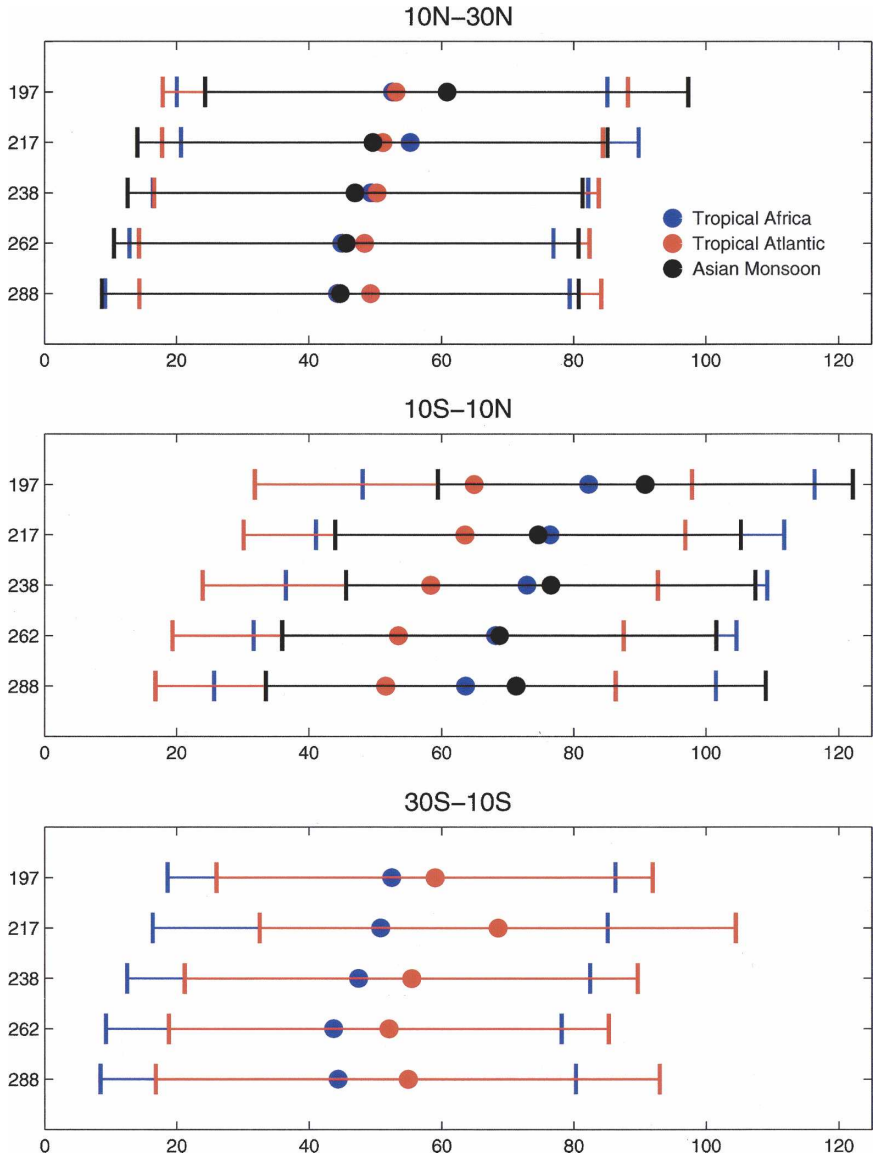

FIG. 3. RHi mean and standard deviation as functions of pressure level and latitudinal zones.

ferences in convective activity and moisture transport. We leave such discussions to section 5 and section 6.

b. *Vertical structure*

Figure 3 shows the height dependence of RHi. Despite a large standard deviation due to the inclusion of different seasons, relative humidity generally increases with height: mean RHi is about 10%–20% (in absolute values) higher at the 197-hPa level than the 288-hPa level. The vertical differences in RHi are usually greater in the deep Tropics than in the subtropics. Although the prominent flight pressure levels vary with region and season and some levels have poorer coverage than others, the values at each pressure level in Fig. 3 are still based on hundreds to thousands of observations so that the statistical basis is strong. We performed a t test for the tropical Atlantic to show this: RHi at 197 hPa is statistically moister than that at 288 hPa at the confidence level higher than 99%, even for a minimum of eight degrees of freedom.

One explanation for the height dependence of UTH is that the upper levels correspond more closely to the convective detrainment layer, where there is an ejection of both saturated air and condensate serving as a moisture source. The lower levels, on the other hand, are subjected more to subsidence drying. The latter ef-

fect can be understood by considering a newly detrained, saturated air parcel undergoing continuous subsidence: since its specific humidity stays constant (when no mixing or condensation occurs), the relative humidity will keep decreasing over the course of the subsidence because of the increase in temperature (Mapes 2001). The mixture of the two mechanisms, namely, convective detrainment and subsidence, can explain the difference between the deep Tropics and subtropics (i.e., the vertical variation of RHi is greater in the deep Tropics than subtropics). In the deep Tropics, both effects exist to enhance the vertical difference in RHi, whereas in the subtropics, convective moistening becomes infrequent and subsidence is left to a large extent to operate alone, thus being less effective in developing a vertical RHi contrast. Detailed observations of the vertical structure of tropical convection (such as from the future CloudSat mission; see Stephens et al. 2002) are needed to verify this conjectured explanation. A cloud-resolving model including all these processes may also be helpful in testing its validity.

The vertical structure of UTH between the 300- and 200-hPa levels has not been well observed by operational radiosondes owing to lack of sensitivity and accuracy at low temperatures, nor by satellites because of the coarse vertical resolution. An increase in UTH from 300 to 200 hPa was detected by some research-quality humidity sensors such as the "Snow White" (e.g., Wang et al. 2003), but these special hygrometers are only used on a limited basis, usually during field campaigns. Thus, Fig. 3 provides a generalized, long-term, near-global observation of the UTH vertical structure. The UTH vertical structure has an important implication for estimating and understanding the earth's radiation budget. To illustrate this, we run a radiative transfer model ("Streamer" by Key 2001) to test the sensitivity of outgoing longwave radiation (OLR) to the variation of moisture between 300 and 200 hPa. Take the Asian monsoon region as an example, where $\mathrm{RHi}_{288\ \mathrm{hPa}} \cong 70\%$ and $\mathrm{RHi}_{197\ \mathrm{hPa}} \cong 90\%$. The difference in OLR assuming constant RHi at the two prescribed values between roughly 300 and 200 hPa is 2.1 W m^{-2} (i.e., 279.4 W m^{-2} for RHi = 90% and 277.3 W m^{-2} for and RHi = 70%), assuming that the rest of the profile follows the Air Force Geophysics Laboratory (AFGL) reference tropical profile (Ellingson et al. 1991). To put this number into perspective, the global mean radiative forcing from anthropogenic CO_2 from year 1750 to 2000 is only 1.5 W m^{-2} (Houghton et al. 2001). In addition to the impact on OLR, UTH also affects the local cooling rate, which, in turn, affects cloud formation and dynamics. A moister upper troposphere tends to push the cooling maximum higher up. For example, the LW cooling rates at 329 and 182 hPa for the McClatchey profile (which is relatively dry in the upper troposphere) are, respectively, 2.2 and 0.81 K day^{-1}, whereas for the same profile everywhere else except the UTH being held constant at RHi of 90% over the 329–182-hPa layer (representing the Asian summer monsoon region), the LW cooling rates now become 1.0 K day^{-1} at 329 hPa and 2.9 K day^{-1} at 182 hPa.

c. UTH probability density function

The probability density function (PDF) of tropical UTH is often bimodal (Zhang et al. 2003). Figure 4 shows the RHi PDFs from MOZAIC sorted by latitude and season (the temporal and spatial resolutions of the data going into the PDFs are 1 min and 15 km). MOZAIC measurements over the tropical Atlantic (Nawrath 2002) and their extension to other tropical regions (Fig. 4) corroborate this important result showing the ubiquitous nature of the bimodality distribution of UTH, although it does not appear as obvious at all locations at all times. Furthermore, they reveal some intriguing details that were not clearly recognized before.

Figure 4 shows that in the deep Tropics (10°S–10°N), the moisture level frequently reaches ice supersaturation and even approaches saturation over liquid water (Nawrath 2002). The most notable case is the Asian monsoon region during the wet season when the UTH distribution almost becomes unimodal at ice saturation in the equator to 10°N band with ice supersaturation observed 46% of the time (the dotted curve in the middle right panel of Fig. 4). The shape of the moist mode is nearly Gaussian, suggesting that processes that generate this mode have equal probability of forming higher or lower RHi about a mean of 100%. Spichtinger et al. (2003) studied the global distribution of ice supersaturation based on the Microwave Limb Sounder (MLS) data, but caution should be exercised when comparing the two UTH datasets. Besides the differences in methodology (i.e., remote sensing versus in situ measurements) and resolution, MLS data should be considered, to a large extent, as clear-sky UTH (Read et al. 2001), whereas the MOZAIC includes measurements from both cloudy and clear conditions. In a different study, we made an attempt to separate cloudy scenes from clear scenes for the MOZAIC measurements using a collocated, high-resolution (5 km and 3 hourly) ISCCP cloud dataset (D. Kley et al. 2006, unpublished manuscript). The other extreme, as depicted in Fig. 4, is in southern Africa during local winter (i.e., boreal summer or JJA) having the driest upper troposphere among all regions with a dry mode at only 10% (the dashed curve in the lower-right panel of Fig. 4). Interestingly, the Sahara region has a much

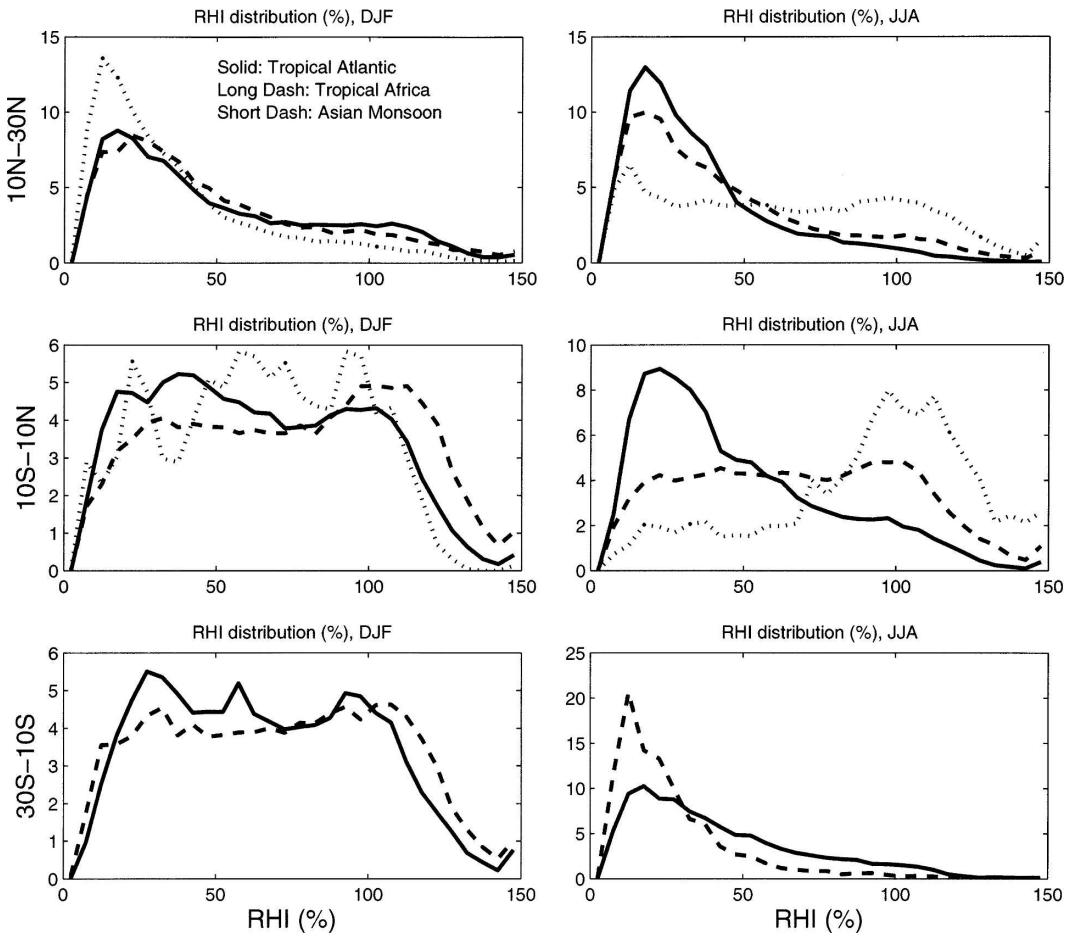

FIG. 4. Probability density functions (in percentage) of RHi (of all five levels) for different latitudinal zones and seasons. Only the boreal winter [December–February (DJF)] and summer [June–August (JJA)] seasons are shown.

wetter upper troposphere than southern Africa: the mean UTH value of the former is about twice as large as the latter (also see Fig. 2).

The two modes in this bimodal distribution stay rather constant; differences in the mean value are largely due to variations in the proportion of the two modes as opposed to changes in modes themselves. Although the bimodal distribution of UTH has been well known (Mapes 2001; Zhang et al. 2003), the relatively constant positions of the two modes have not been clearly recognized (with the notable exception of Nawrath 2002). This suggests that the two dominant modes are probably a manifestation of two key processes that have controlling effects on UTH, presumably convection (moistening) and subsidence (drying); each process has its associated characteristic UTH. The "valleys" in between the two modes are probably related to the mixing processes that tend to homogenize the UTH distribution. Mixing is shown to have a longer characteristic time (thus a slower process) than subsidence drying (and probably convective moistening too) in the tropical upper troposphere (Zhang et al. 2003). If mixing were fast enough, there would not be any valley nor the bimodal distribution in the first place.

Although this study is mainly about the Tropics, a little discussion of the midlatitude UTH distribution may help illuminate the problem. In midlatitudes, the MOZAIC UTH gives a unimodal distribution broadly centered between RHi of 50% and 100% (Nawrath 2002); the frequency for ice supersaturation is comparable to that of the Tropics, but the dry mode is largely gone. Satellite observations show a consistent picture: if one looks at an instantaneous water vapor imagery from satellite (usually measuring the radiance around the 6.7-μm spectrum), it will be noticed that the transition from moist to dry areas is usually sharper and the moisture gradient is stronger in the Tropics than the midlatitudes. Along the same line of argument, this unique UTH distribution in midlatitudes can be considered a reflection of the characteristics of the dominant

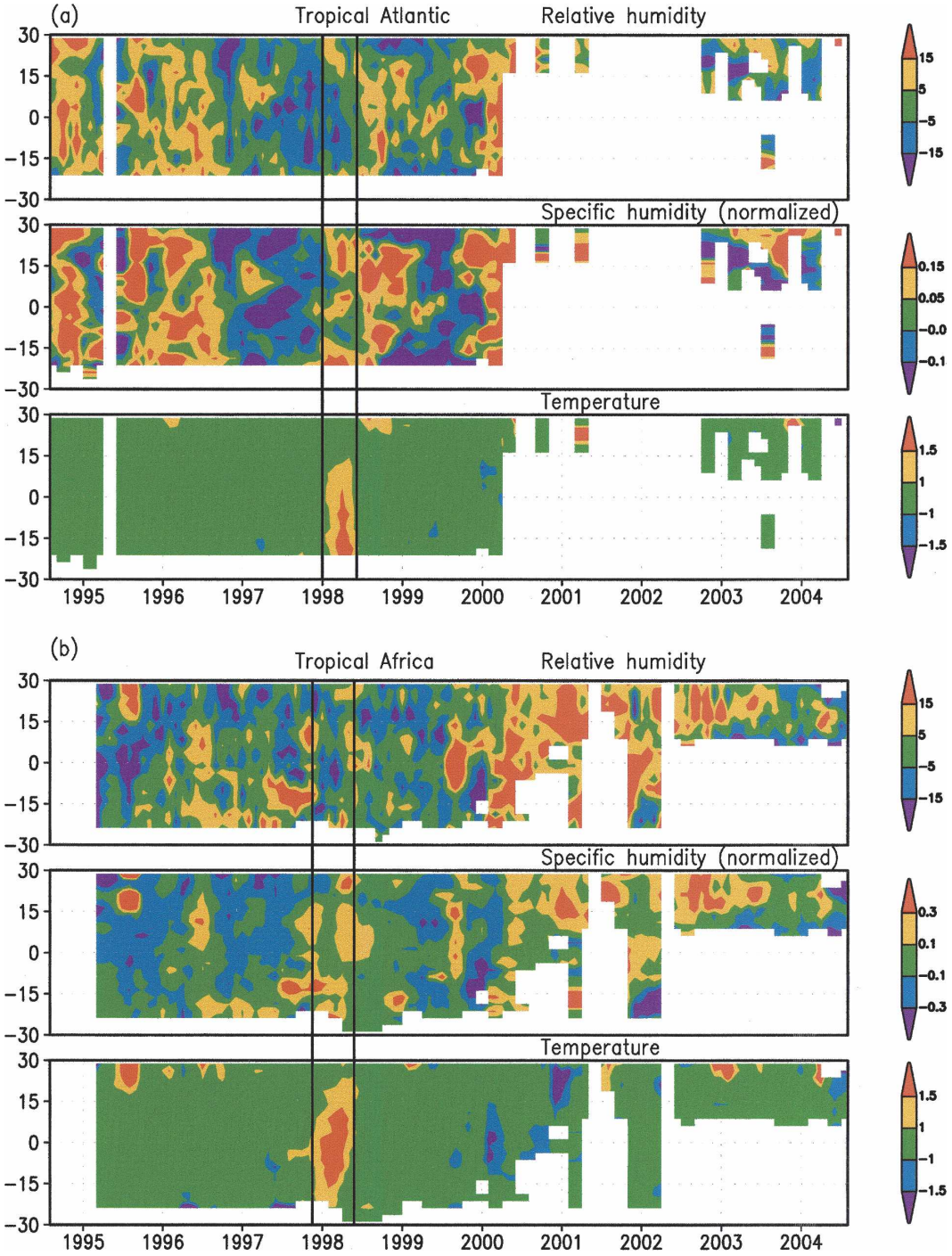

FIG. 5. Interannual variations of monthly mean RHi, specific humidity, and temperature with annual cycles removed for (a) the tropical Atlantic, (b) tropical Africa, and (c) the Asian monsoon region. To accommodate all five flight levels, the specific humidity is normalized by the corresponding mean values at each level.

processes controlling it. In midlatitudes, the radiative-driven subsidence is weaker and slower than in the Tropics due to less water vapor load in the atmosphere. Unlike the Tropics, the slower drying process probably cannot overtake the mixing to maintain a local dry condition. Of course, it is also possible that the flight levels of the MOZAIC aircraft in midlatitudes are closer to the tropopause and hence air is subjected less to subsidence. Whichever the case, subsidence is a crucial process to the distribution of UTH.

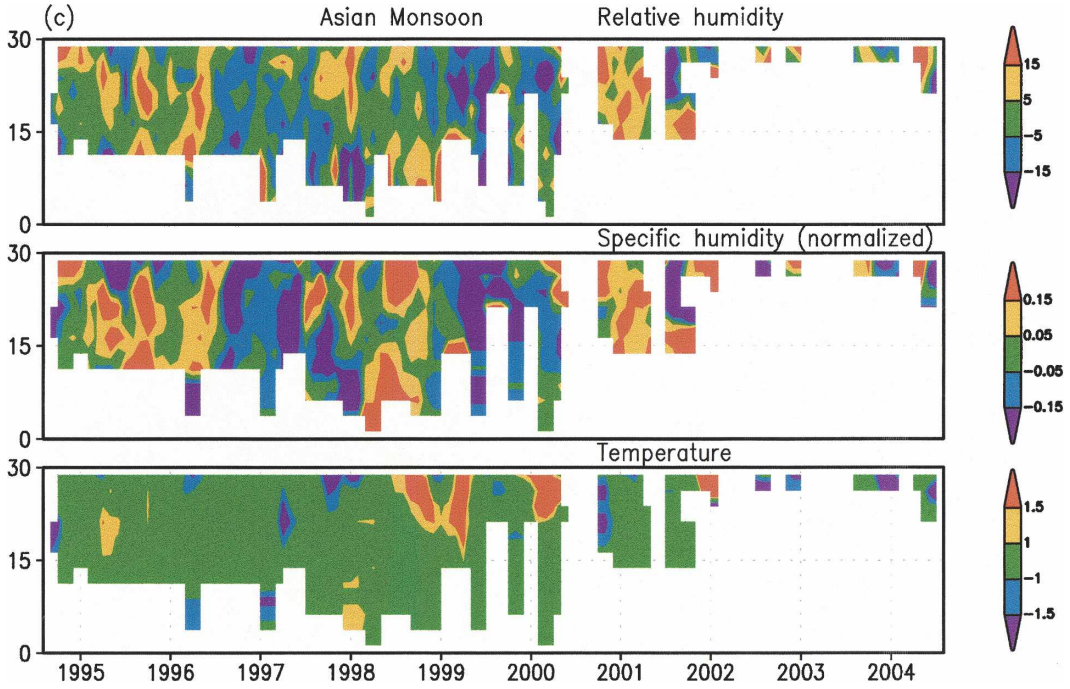

FIG. 5. (*Continued*)

4. Interannual variability

An analysis of interannual variability in UTWV can be made with the MOZAIC data due to the fact that the same instrumentation with known and assured accuracy is used throughout. The 10-yr period is of course not long enough to conclusively establish climate trends, but it is worth investigating whether any interannual variation can be detected in the data record. The near-global nature of the MOZAIC data also makes such an analysis unique in that the variability can be studied for more than one region.

Figure 5 shows the monthly mean UTH (in RHi) variations as a function of latitude and time for the period from 1994 to 2004; seasonal cycles, as shown in Fig. 2, have been removed. Also shown are the interannual variations of specific humidity and temperature from MOZAIC flight data. Since specific humidity and its variability decrease sharply with height, we normalize it by the level-mean value to include measurements from all five flight levels (to maximize data coverage). The normalized variation of specific humidity (in terms of fractional changes) stays roughly constant across all five flight levels (Nawrath 2002). In contrast, the vertical dependence of variations in temperature and relative humidity is very small, so no normalization is needed. A 3-month averaging window is applied to the original data to smooth out some sporadic discontinuities in measurements. Some large gaps, however, still exist, especially for the tropical Atlantic and the Asian monsoon region from mid-2000 to early 2004 owing to increased deployment of the five MOZAIC aircraft to the regions outside of the Tropics (the majority of the MOZAIC flights cover areas in midlatitudes).

In general, upper-tropospheric temperature experiences little temporal variation, whereas moisture variability (both specific humidity and relative humidity) is large. The small temperature perturbation thus makes relative humidity variation closely follow that of the specific humidity, as shown in Fig. 5. But this rule breaks down during ENSO. For the period of the 1997–98 ENSO, there is a significant warming of about 1–2 K for all three regions equatorward of roughly 15°[3] and the variation of specific humidity is decoupled from that of RH: Figs. 5a and 5b (over the tropical Atlantic and tropical Africa) show that overall, as the temperature rises during the ENSO, specific humidity also increases somewhat, but the increase in temperature (which tends to decrease RH) outweighs the increase in specific humidity (which tends to increase RH) such that RH decreases by 5%–15% RHi. The signal in the Asian summer monsoon region (Fig. 5c) is less clear due to the scarcity of observation at low latitude.

McCarthy and Toumi (2004) studied the interannual variability of all three fields (i.e., temperature, RH, and specific humidity) using a satellite-based UTH product

[3] Note that the Asian monsoon region only includes areas north of the equator, so the signal is less obvious from the figure.

derived from the High-Resolution Infrared Sounder (HIRS) channel-12 brightness temperature and the National Centers for Environmental Prediction–National Center for Atmospheric Research (NCEP–NCAR) reanalysis data. Their composite ENSO-related variations of upper-tropospheric temperature and humidity (both specific and relative) are similar to the MOZAIC results; that is, the increase in temperature dominates the increase in specific humidity, resulting in a decrease in RH by about 5%–10% RHi, over the tropical Atlantic and tropical Africa regions. Because the tropical free atmosphere cannot maintain large horizontal temperature gradients, the ENSO warming of the troposphere is widespread and rather uniform over the whole Tropics (Yulaeva and Wallace 1994; Chiang and Sobel 2002), contributing negatively to the RH variation almost everywhere. Changes in specific humidity, on the other hand, are controlled by the shift of SST patterns and the associated changes in convection, which tend to be much patchier than the fairly uniform warming of the atmosphere (McCarthy and Toumi 2004). The net effect of ENSO on UTH therefore differs from place to place. Averaged over the whole Tropics, UTH seems to decrease by a little with the ENSO warming (Sun and Oort 1995, Minschwaner and Dessler 2004), but the range does not exceed a few percent.

In addition to the ENSO-related variations, Fig. 5b also shows an increase in UTH over tropical Africa from around 2000 to 2002, and probably beyond. The increase in UTH mainly comes as a result of the rise in specific humidity level rather than changes in temperature. The reason for this African moistening is not clear and has not been previously documented, to the authors' knowledge. Since a minimum of three flights (which give hundreds, if not thousands, of measurements) are required for each month to generate the monthly mean statistics (otherwise it will be labeled as having missing data) and this increase is not short-lived but lasts for over two years, it is unlikely to be a sampling artifact. Moreover, there is no known problem with the measurement quality that can explain this change. More studies are needed to unravel the nature of the African moistening.

5. MOZAIC moisture fluxes and transport[4]

The spatial distribution of UTWV is controlled by the interplay of a number of processes. Among them, horizontal transport or advection plays an important role, especially in determining the UTWV climatology in the convection-free regions (Sherwood 1996). Previous studies of the UTWV horizontal transport use data from the following three sources: rawinsonde (e.g., Peixoto and Oort 1992), satellite (e.g., Soden 1998), and reanalysis (e.g., Pierrehumbert and Roca 1998). In this section, we make use of the MOZAIC measurements as an alternative data source to study the upper-tropospheric moisture fluxes and transport, taking advantage of the fact that both specific humidity and flight-level winds are readily obtainable from the MOZAIC aircraft.

Figure 6 shows the seasonal- and zonal-mean moisture fluxes at the 238-hPa level. We choose the 238-hPa level because it is a prominent flight level common to all three tropical regions containing most measurements. The moisture flux patterns are similar at other levels (not shown), but the magnitude differs from one level to another mainly due to the rapid decrease of water vapor mixing ratio with height. Some well-known tropical upper-tropospheric circulation patterns and the associated moisture transport are readily identified in Fig. 6. The subtropical westerly jet is frequently observed during the local winter centered between the 20° and 30° latitude. The tropical easterly jet is seen during local summer equatorward of 10° latitude (most obvious over the tropical Africa). The upper-tropospheric branch of the Asian summer monsoon circulation is also well depicted with reversing wind direction between summer and winter seasons.

Note that what is shown in Fig. 6 is not just mean winds of the tropical upper troposphere (which is nothing new), but the product of winds and specific humidity. To emphasize the difference, we compare, over tropical Africa, the subtropical westerly jet and tropical easterly jet as well as the associated moisture fluxes (see the middle panel of Fig. 6): in terms of wind speed alone, the subtropical westerly jet is about five times stronger than the tropical easterly jet (i.e., 50 versus 10 $m\ s^{-1}$), but the contrast is largely reduced or even reversed when it comes to moisture fluxes because the deep Tropics, although having weaker winds than the subtropics, is also a lot wetter than the subtropics. Accurate depiction of upper-tropospheric moisture fluxes is a challenging task for the three previously used data sources (i.e., rawinsondes, satellites, and reanalysis) because none of them can provide simultaneous, accurate measurements of both upper-tropospheric winds and moisture. Rawinsonde moisture data suffer from the loss of sensitivity and accuracy at cold temperatures, which is why such studies are usually limited to below

[4] Note that total moisture transport should include both the horizontal and vertical fluxes. Vertical fluxes cannot be directly measured from the MOZAIC aircraft, but their contribution will be estimated from horizontal flux divergence.

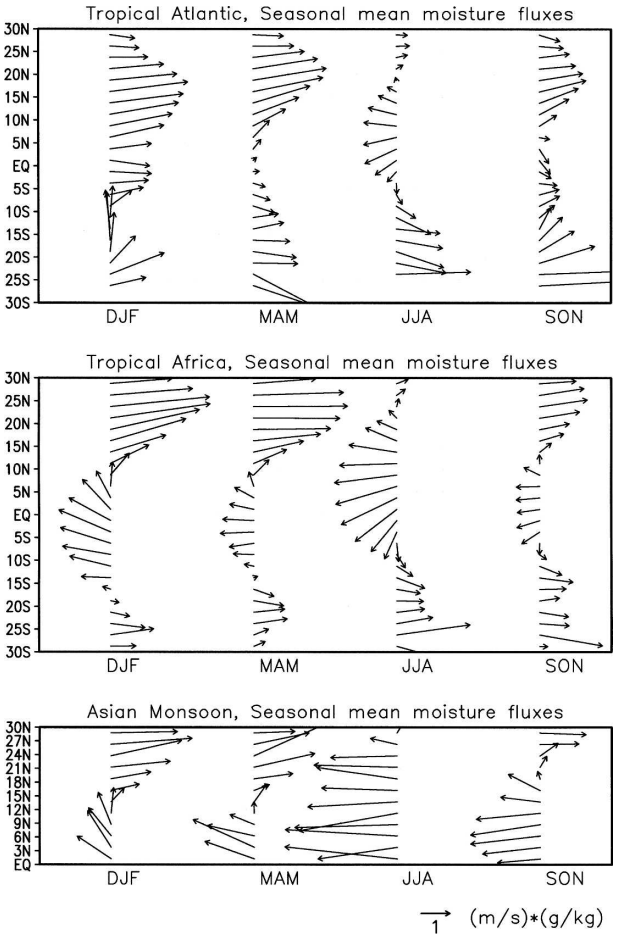

FIG. 6. Composite annual cycle of moisture fluxes at the 238-hPa level.

300 hPa (e.g., Sun and Oort 1995). Satellite measurements are affected by their coarse vertical resolution and cloud contamination problem. Reanalysis winds, on the other hand, have a relatively poor quality in the Tropics owing to the lack of upper-air data and dynamic constraint in low latitudes; so does the reanalysis moisture field, which is sensitive to the convection and cloud parameterizations used in the data assimilation system. MOZAIC-derived moisture fluxes can overcome many of these difficulties and provide long-term, near-global, high-quality, in situ measurements of this important quantity, which can serve as a benchmark for model comparison studies [in a companion paper, we use the MOZAIC data as a comparison basis for evaluating the European Centre for Medium-Range Weather Forecasts (ECMWF) product]. Nevertheless, there are issues with the MOZAIC data as well. Since aircraft fly across the Atlantic roughly twice per week and less frequently over other regions, moisture transports by eddies on a shorter time scale could be missed. But 10 yr of data can help mitigate the problem since long-term averages smear out some effects of the short-term eddies.

In addition to the total moisture fluxes, we also make an attempt to decompose them into contributions from the mean circulation and from eddies. A breakdown of moisture fluxes into these components helps one understand the roles of general circulation and transient motions in influencing the moisture transport (Peixoto and Oort 1992). If we define $v = \bar{v} + v'$ and $q = \bar{q} + q'$, where the overbar and prime terms refer to, respectively, the annual means and the deviations (i.e., eddies), then following Peixoto and Oort (1992) we get $\overline{vq} = \bar{v}\bar{q} + \overline{v'q'}$. The first term on the right-hand side is the contribution from the mean circulation, whereas the second term is the contribution from eddies. By eddies, we mean all moisture transports on the time scale shorter than a year, including daily, weekly, intraseasonal, and seasonal scales. For the reason discussed above, eddies on the daily scale may be largely missed. Nevertheless, the results still have their value because, to our knowledge, such a flux decomposition has not been documented at the upper-tropospheric level between 300 and 200 hPa. Peixoto and Oort (1992) used rawinsonde data to estimate the mean versus eddy contributions, but because of the loss of sensitivity and accuracy at cold temperatures, their results are cut off around 300 hPa (see, e.g., their Fig. 12.11). It is our future plan to assess the importance of what is being missed in a separate study by going into a high temporal-resolution model and subsampling the fluxes on the MOZAIC time scales and comparing those values with the fluxes obtained from higher resolutions of the model. Figure 7 shows the annual-mean moisture fluxes and the corresponding decomposition into contributions from mean circulation and eddies. Zonal fluxes and meridional fluxes are shown separately. Several findings deserve discussion. 1) *Zonal fluxes:* over the tropical Atlantic and tropical Africa, mean circulation makes a dominant contribution to the total zonal fluxes; over the Asian monsoon region, however, the eddy contribution becomes an important part, especially around the subtropics from 15° to 30°N, due to the unique circulation pattern of the monsoon (which is considered as eddies in this study). Note that eddy transports over the Asian monsoon region tend to oppose those by the mean circulation. 2) *Meridional fluxes*: eddies generally make a larger proportional contribution to the total meridional fluxes than to the total zonal fluxes. This is especially the case over the tropical Atlantic and tropical Africa around the subtropical regions where eddies tend to transport moisture from the

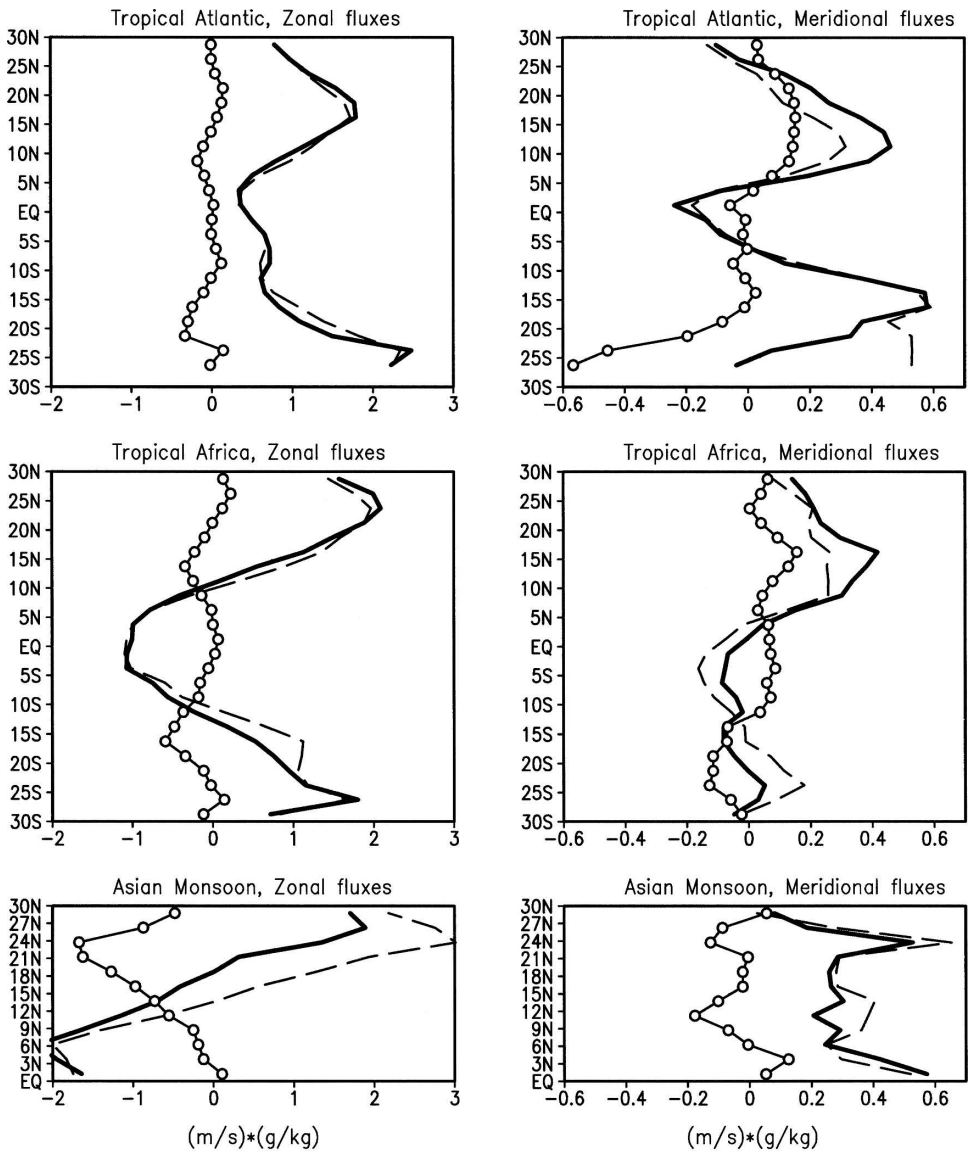

FIG. 7. Decomposition of the total moisture fluxes into contributions from the mean circulation and from eddies: (left) zonal fluxes and (right) meridional fluxes. Note that the mean circulation refers to the annual mean and that eddies include all moisture transport on any time scale shorter than that.

deep Tropics to the subtropics. The Asian summer monsoon region is again different, where eddies move moisture from the subtropics to the deep Tropics in association with the unique circulation of the Asian monsoon.

Moisture flux measures the water vapor transport by the atmospheric circulation, but it is the divergence of the flux that really determines the net source or sink of water vapor through transport. To derive the flux divergence, one has to know the spatial distribution of the fluxes. This may be a little difficult for the MOZAIC data as the flight corridors usually cover some narrow "lines" (see Fig. 1). Nevertheless, we can still get a composite depiction of the moisture flux divergence based on nearly 10 yr of data. Figure 8 shows the seasonal composite of horizontal moisture flux divergence for the three tropical regions. The spatial resolution for diagnosing the flux divergence is 2.5°, roughly the size of the present-day GCM grid boxes. Unlike moisture fluxes, the divergence of these fluxes is a little

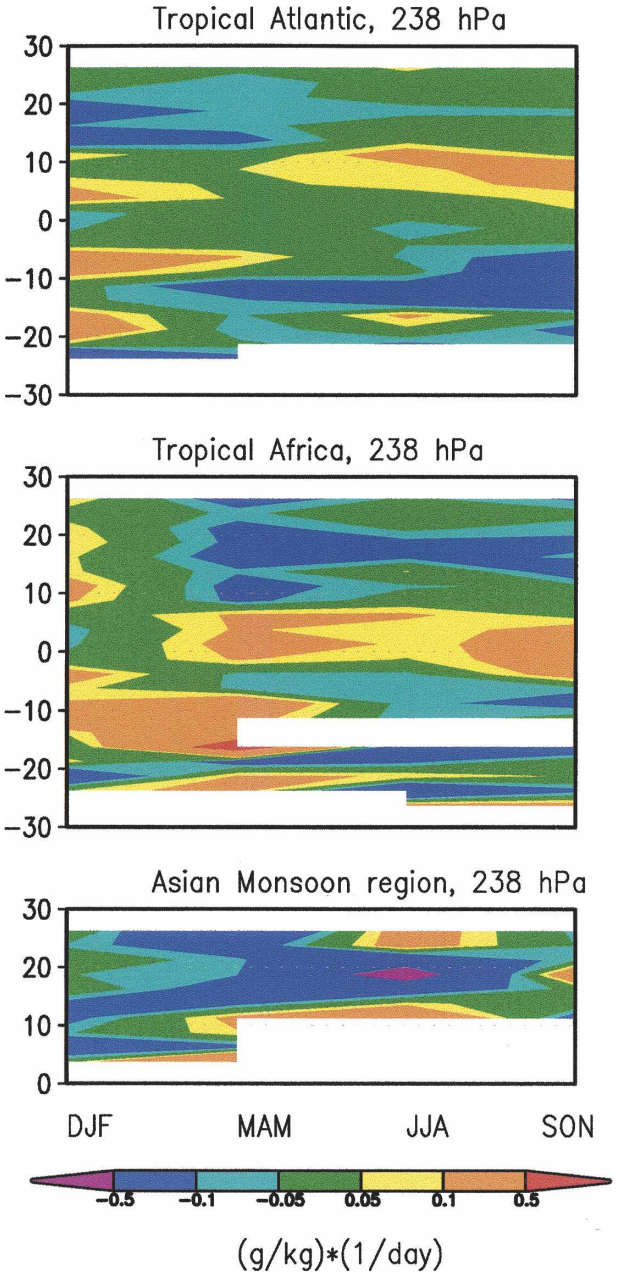

FIG. 8. Composite annual cycle of moisture flux divergence at the 238-hPa level.

"noisy," but some climatologically significant patterns are still clearly seen. Comparing Fig. 2 with Fig. 8 shows that the moist regions are usually associated with horizontal moisture divergence (positive contours) exporting water vapor to the neighboring regions. Therefore, horizontal transport is a local water vapor sink in these regions that must be balanced by moistening processes such as vertical transport associated with convection. Dry regions, on the other hand, are associated with moisture convergence (negative contours); water vapor transport thus becomes a local source balancing the subsidence drying. These results are consistent with the previous study of the source and sink of the free tropospheric water vapor by Sherwood (1996) using reanalysis data, although Sherwood's results are limited to below 300 hPa.

6. Relation to deep convection

Deep convection has a profound influence on the distribution of the UTWV (Soden and Fu 1995; Udelhofen and Hartmann 1995; Salathe and Hartmann 1997). In this section, the MOZAIC climatology and variability are revisited in relation to deep convection. The ISCCP data are used to describe tropical deep convection.

ISCCP retrieves cloud properties from analyzing infrared (~11 μm) and visible (~0.6 μm) radiances measured by the imaging instruments on all of the available operational weather satellites. The visible channel is useful in estimating cloud optical depth and assigning cloud top height for nonopaque clouds (such as thin cirrus), but it limits the application to daytime only. Since we are only concerned with deep convective clouds in general, the infrared channel alone is sufficient for singling them out (Luo and Rossow 2004). The ISCCP D1 data are used in this study; the temporal resolution of the data is 3 h and the spatial resolution is about 280 km. Two infrared-only cloud types are most relevant to the MOZAIC measurements: high clouds with cloud-top pressure between 310 and 180 hPa (referred to as convection type I) and those with cloud top pressure lower than 180 hPa (referred to as convection type II), which correspond to the temperature (height) of roughly 240 (9.5 km) and 220 K (12 km), respectively. Figure 9 shows the long-term (1994–2004, matching the MOZAIC period) climatology of the type-I convection. In the Tropics, clouds with infrared-only tops[5] at this altitude are almost solely associated with deep convective plumes and their thick anvils. Thin cirrus will not show up as cold in the infrared channel because their semitransparent nature allows a fraction of the radiation from below to reach the satellite sensor, making them appear as warmer clouds. For this reason, we use the ISCCP infrared-only high cloud frequency as a proxy for convective frequency (note that this method may not work for identifying convective clouds in mid-

[5] Infrared-only top refers to the cloud top determined by simply inverting the observed brightness temperature. Cloud tops defined this way are always equal to or lower than the physical cloud tops.

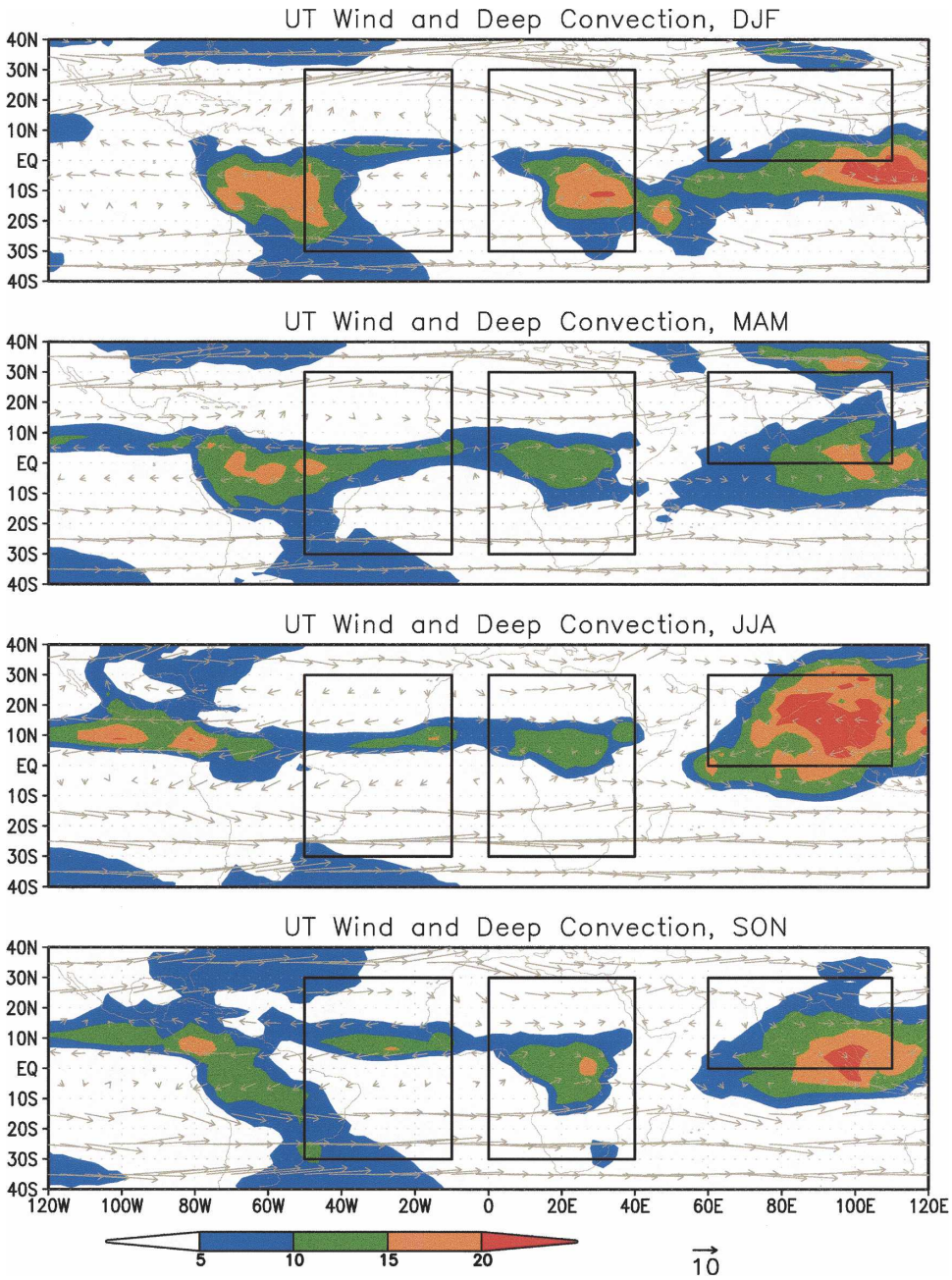

FIG. 9. Long-term (1994–2004) climatology of the ISCCP convection type I (contours in percentage) and the 250-hPa winds from the NCEP–NCAR reanalysis: (from top to bottom) the DJF, MAM, JJA, and SON seasons.

latitudes, where high cloud tops are often associated with extratropical cyclones, especially during the winter season). Superimposed in Fig. 9 are also the climatological 250-hPa winds taken from the NCEP–NCAR reanalysis. Figure 9 shows that the regional differences in MOZAIC UTH climatology (Figs. 2 and 4) are closely connected to the differences in the distribution of deep convection. For example, the tropical Atlantic has the driest upper troposphere because it has the least amount of deep convection reaching the upper-tropospheric levels where MOZAIC measurements are made. The Asian monsoon region, on the other hand, has the moistest upper troposphere during the wet season and also the most abundant deep convection. Tropical Africa comes in between in terms of convective frequency and UTH level.

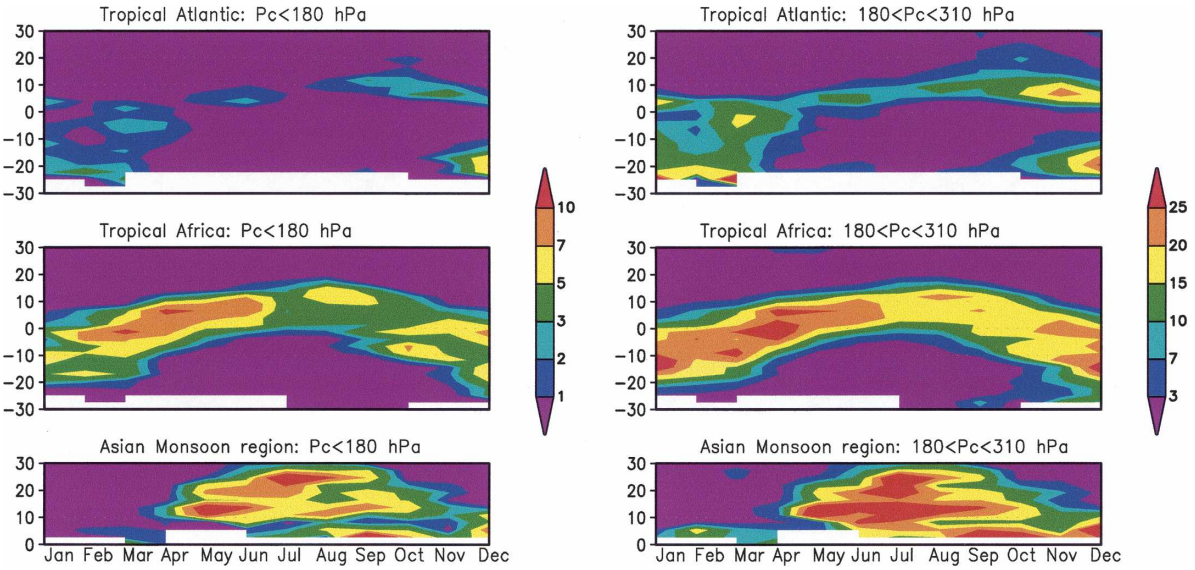

FIG. 10. Composite annual cycle of the two ISCCP types of convection (cf. Fig. 2).

Following Fig. 2, we construct a composite annual cycle for the ISCCP deep convection (Fig. 10). ISCCP has much denser temporal and spatial coverage (3 h and 30 km) than the MOZAIC data, but we only sample it where MOZAIC measurements were made to ensure an unbiased comparison with Fig. 2. Both types of convection are shown; their patterns are similar although convection type II with higher tops (and probably greater strength) is less frequently observed. The composite annual cycle of deep convection very much resembles that of the UTH (Fig. 2), indicating the importance of vertical transport by deep convection to UTH. The regional differences in UTH are manifested in the convective frequency difference. Compared to convection, the UTH pattern is more diffuse and exhibits weaker gradient because moisture transports move water vapor from convective regions to dry regions, blurring the boundary between them. Table 1 quantifies the similarity between the two annual cycles by showing the correlations between them for three latitudinal zones. In general, the correlation coefficients between convection type I (180 hPa $< P_c <$ 310 hPa) and UTH are larger than those between convection type II ($P_c <$ 180 hPa) and UTH, suggesting that convection type I may have a greater influence on UTH measured by the MOZAIC aircraft. This makes sense because MOZAIC flight levels in the Tropics cover from 288 to 197 hPa, roughly the height range of the convection type-I cloud tops. In addition to annual cycle, we also calculate the interannual variation (with annual cycle removed) of the ISCCP convective frequency and compare it to that of the MOZAIC UTH (Table 2). In contrast to the correlations between annual cycles, interannual variation of deep convection is less well correlated with that of UTH. This suggests that factors other than deep convection (such as changes in moisture transport and large-scale dynamics) probably also play an important role in determining the interannual variation of UTH over these regions.

7. Summary and Conclusions

Ten years (1994–2004) of measurements of tropical upper-tropospheric water vapor (UTWV) by MOZAIC are investigated over three selected regions: tropical Atlantic, tropical Africa, and the Asian monsoon region. The overarching goals are to determine the UTWV climatology and variability on multiple scales and to understand them in relation to moisture trans-

TABLE 1. Correlations between the composite annual cycles of the MOZAIC RHi (Fig. 2) and the ISCCP convection (Fig. 10). Convection type I (180 hPa $< P_c <$ 310 hPa) and type II ($P_c <$ 180 hPa) are correlated with RHi separately. A t test is performed to determine the significance level of the correlation coefficients. All correlations with a significance level of 1% are bold.

	Tropical Atlantic		Tropical Africa		Asian monsoon region	
	Type I	Type II	Type I	Type II	Type I	Type II
10°–30°N	**0.80**	0.26	−0.37	−0.54	**0.93**	**0.86**
10°S–10°N	**0.92**	**0.76**	0.63	0.35	**0.65**	0.46
30°–10°S	**0.91**	**0.80**	**0.97**	**0.95**		

TABLE 2. As in Table 1 except that the correlations are calculated for the interannual variations (with annual cycle removed).

	Tropical Atlantic		Tropical Africa		Asian monsoon region	
	Type I	Type II	Type I	Type II	Type I	Type II
10°–30°N	**0.49**	0.19	0.16	0.02	0.26	0.17
10°S–10°N	**0.70**	**0.44**	0.28	0.29	**0.65**	0.44
30°–10°S	0.43	0.31	**0.80**	**0.68**		

port and deep convection. MOZAIC provides a unique opportunity to approach these goals because of its high accuracy, high resolution, and long-term/near-global coverage. In a companion paper, we also use it as a comparison basis for evaluating the ECMWF product.

Based on nearly 10 yr of data, the composite annual cycle of upper-tropospheric humidity (UTH) is constructed. The UTH annual cycle keeps pace with the corresponding seasonal migration of the ITCZ, highlighting the convective influence on UTH distribution. Some significant regional differences are identified: the moistest upper-troposphere is found in the Asian monsoon region during the wet season (with the monthly mean RH exceeding ice saturation), followed by tropical Africa during the local summer, while it is least likely to see very moist conditions in the tropical Atlantic. Relative humidity in the tropical upper troposphere generally increases with height by 10%–20% RHi from about 300 to 200 hPa, and the difference is larger in the deep Tropics than in the subtropics. We explain the vertical structure of UTH as the result of the combined effects of convective detrainment (moistening) and radiatively driven subsidence (drying). UTH vertical structure is shown to have a significant impact on the earth's radiation budget and the local cooling rate.

The probability density function of tropical UTH from MOZAIC is often bimodal, as suggested by a number of previous studies. Some intriguing details pertaining to this bimodality are uniquely identified by the MOZAIC data. In the deep Tropics, the moisture level frequently reaches ice supersaturation and even approaches saturation over liquid. The most notable example is the Asian monsoon region equatorward of 10°, where ice supersaturation is observed 46% of the time during the wet season. The two modes in this bimodal distribution stay rather constant: differences in the mean value are largely due to variations in the proportion of the two modes as opposed to changes in the modes themselves. This suggests that the two dominant modes are probably a manifestation of two key processes having controlling effects on UTH, presumably deep convection and subsidence; each process has its associated characteristic UTH. In comparison, mixing (which tends to homogenize the UTH distribution) must have a longer characteristic time (thus a slower process).

Interannual variations of UTH, specific humidity, and temperature are studied. Some noticeable variations are associated with the 1997–98 ENSO event: a warming of about 1–2 K is observed for all three regions equatorward of roughly 15°, and at the same time, specific humidity also rises somewhat for the tropical Atlantic and tropical Africa, but the increase in temperature outweighs the increase in specific humidity such that RH decreases by 5%–15% RHi. In addition to the ENSO-related variations, there is an intriguing moistening observed over tropical Africa from 2000 to 2002 (and probably beyond). The reason for the moistening is unknown and it has not been previously documented, either, to the authors' knowledge. More study is needed.

Meridional and zonal moisture fluxes as measured onboard the MOZAIC aircraft are examined. Some well-known tropical upper-tropospheric circulation patterns are readily identified, including the subtropical westerly jet, tropical easterly jet, monsoon circulations, and meridional overturning cell. Because moisture levels are different among these circulation patterns, the associated moisture fluxes are very different from the mean winds (e.g., the tropical easterly jet region, although having much lighter winds than the subtropical westerly jet region, is also much wetter). The total moisture fluxes are further decomposed into contributions from the mean circulation and from eddies. The divergence of moisture fluxes (which represents the moisture source/sink due to horizontal advection) is also calculated. The moist regions are usually associated with horizontal moisture divergence exporting water vapor to the neighboring regions. Dry regions, on the other hand, are associated with moisture convergence.

Finally, the MOZAIC climatology and variability are revisited in relation to deep convection. ISCCP infrared-only high cloudiness is used as a proxy for deep convection. The regional differences in the UTH annual cycle are shown to be closely related to the differences in convective frequency. The interannual variation of UTH is also manifested in the changes in convection, but to a lesser extent than the annual cycles.

Acknowledgments. This work was supported by the National Science Foundation (NSF) under Grant ATM-0444244. We thank Air Fance, Austrian Airlines, Lufthansa, and Sabena for carrying the MOZAIC

equipments on scheduled flights and handling regular installation/de-installation of the humidity sensors. The first author (Luo) would like to thank Dr. Graeme Stephens at Colorado State University for his continuous support and insightful discussion. Thanks are also due to two anonymous reviewers for their helpful comments.

REFERENCES

Bates, J. J., X. Wu, and D. L. Jackson, 1996: Interannual variability of upper-tropospheric water vapor band brightness temperature. *J. Climate,* **9,** 427–438.

Cess, R. D., and Coauthors, 1990: Intercomparison and interpretation of climate feedback processes in 19 atmospheric general circulation models. *J. Geophys. Res.,* **95,** 16 601–16 615.

Chiang, J. C. H., and A. H. Sobel, 2002: Tropical tropospheric temperature variations caused by ENSO and their influence on the remote tropical climate. *J. Climate,* **15,** 2616–2631.

Ellingson, R. G., J. Ellis, and S. Fels, 1991: The intercomparison of radiation codes in climate models: Long wave results. *J. Geophys. Res.,* **96,** 8929–8953.

Elliot, W. P., and D. J. Gaffen, 1991: On the utility of radiosonde humimdity archives for climate studies. *Bull. Amer. Meteor. Soc.,* **72,** 1507–1520.

Gierens, K., and P. Spichtinger, 2000: On the size distribution of ice-supersaturated regions in the upper troposphere and lowermost stratosphere. *Ann. Geophys.,* **18,** 499–504.

——, U. Schumann, M. Helten, H. Smit, and A. Marenco, 1999: A distribution law for relative humidity in the upper troposphere and lower stratosphere derived from three years of MOZAIC measurements. *Ann. Geophys.,* **17,** 1218–1226.

Held, I., and B. J. Soden, 2000: Water vapor feedback and global warming. *Annu. Rev. Energy Environ.,* **25,** 441–475.

Helten, M., H. G. J. Smit, W. Sträter, D. Kley, P. Nedelc, M. Zöger, and R. Busen, 1998: Calibration and performance of automatic compact instrumentation for the measurement of relative humidity from passenger aircraft. *J. Geophys. Res.,* **103,** 25 643–25 652.

——, and Coauthors, 1999: In-flight intercomparison of MOZAIC and POLINAT water vapor measurements. *J. Geophys. Res.,* **104,** 26 087–26 096.

Houghton, J. T., Y. Ding, D. J. Griggs, M. Noguer, P. J. van der Linden, X. Dai, K. Maskell, and C. A. Johnson, Eds., 2001: *Climate Change 2001: The Scientific Basis.* Cambridge University Press, 881 pp.

Key, J., 2001: Streamer version 3.0 user and reference guides. Cooperative Institute for Meteorological Satellite Studies, University of Wisconsin—Madison, 70 pp.

Kley, D., J. M. Russel III, and C. Phillips, Eds., 2000: SPARC assessment of upper tropospheric and stratospheric water vapor. WCRP-No113, WMO/TD-No1043, SPARC Rep. 2, 312 pp. [Available online at http://www.atmosp.physics.utoronto.ca/SPARC/WAVASFINAL_000206/WWW_wavas/Cover.html.]

Lindzen, R. S., 1990: Some coolness concerning global warming. *Bull. Amer. Meteor. Soc.,* **71,** 288–299.

Luo, Z., and W. B. Rossow, 2004: Characterizing tropical cirrus life cycle, evolution, and interaction with upper-tropospheric water vapor using Lagrangian trajectory analysis of satellite observations. *J. Climate,* **17,** 4541–4563.

Mapes, B. E., 2001: Water's two height scales: The moist adiabat and the radiative troposphere. *Quart. J. Roy. Meteor. Soc.,* **127,** 2353–2366.

Marenco, A., and Coauthors, 1998: Measurement of ozone and water vapor by Airbus in-service aircraft: The MOZAIC airborne program, an overview. *J. Geophys. Res.,* **103,** 25 631–25 642.

McCarthy, M., and R. Toumi, 2004: Observed interannual variability of tropical troposphere relative humidity. *J. Climate,* **17,** 3181–3191.

Minschwaner, L., and A. E. Dessler, 2004: Water vapor feedback in the tropical upper troposphere. *J. Climate,* **17,** 1272–1282.

Nawrath, S., 2002: Water vapor in the tropical upper troposphere: On the influence of deep convection. Ph.D. thesis, Universität Köln, Cologne, Germany, 104 pp. [Available online at http://kups.ub.uni-koeln.de/volltexte/2003/411/.]

Peixoto, J. P., and A. H. Oort, 1992: *Physics of Climate*. American Institute of Physics, 520 pp.

Pierrehumbert, R. T., and R. Roca, 1998: Evidence for control of Atlantic subtropical humidity by large scale advection. *Geophys. Res. Lett.,* **25,** 4537–4540.

——, H. Brogniez, and R. Roca, 2005: On the relative humidity of the Earth's atmosphere. *The Global Circulation of the Atmosphere: Phenomena, Theory, Challenges,* T. Schneider and A. H. Sobel, Eds., Princeton University Press, in press.

Pope, V. D., J. A. Pamment, R. Jackson, and A. Slingo, 2001: The representation of water vapor and its dependence on vertical resolution in the Hadley Centre Climate Model. *J. Climate,* **14,** 3065–3085.

Read, W. G., and Coauthors, 2001: UARS Microwave Limb Sounder upper tropospheric humidity measurement: Method and validation. *J. Geophys. Res.,* **106,** 32 207–32 258.

Rossow, W. B., and R. A. Schiffer, 1999: Advances in understanding clouds from ISCCP. *Bull. Amer. Meteor. Soc.,* **80,** 2261–2287.

Salathe, E. P., and D. L. Hartmann, 1997: A trajectory analysis of tropical upper-tropspheric moisture and convection. *J. Climate,* **10,** 2533–2547.

Sherwood, S. C., 1996: Maintenance of free-tropospheric tropical water vapor distribution. Part I: Clear regime budget. *J. Climate,* **9,** 2903–2918.

Soden, B. J., 1998: Tracking upper tropospheric water vapor radiances: A satellite perspective. *J. Geophys. Res.,* **103,** 17 069–17 081.

——, 2004: The impact of tropical convection and cirrus on upper tropospheric humidity: A Lagrangian analysis of satellite measurements. *Geophys. Res. Lett.,* **31,** L20104, doi:10.1029/2004GL020980.

——, and F. P. Bretherton, 1993: Upper tropospheric relative humidity from the GOES 6.7 μm channel: Method and climatology for July 1987. *J. Geophys. Res.,* **98,** 16 669–16 688.

——, and R. Fu, 1995: A satellite analysis of deep convection, upper-tropospheric humidity, and the greenhouse effect. *J. Climate,* **8,** 2333–2351.

Spichtinger, P., K. Gierens, and W. Read, 2003: The global distribution of ice-supersaturated regions seen by the Microwave Limb Sounder. *Quart. J. Roy. Meteor. Soc.,* **129,** 3391–3410.

Stephens, G. L., D. L. Jackson, and I. Wittmeyer, 1996: Global observations of upper-tropospheric water vapor derived from TOVS radiance data. *J. Climate,* **9,** 305–326.

——, and Coauthors, 2002: The CloudSat mission and the A-Train: A new dimension of space-based observations of clouds and precipitation. *Bull. Amer. Meteor. Soc.,* **83,** 1771–1790.

Sun, D.-Z., and A. Oort, 1995: Humidity–temperature relationships in the tropical troposphere. *J. Climate,* **8,** 1974–1987.

Thouret, V., A. Marenco, P. Nédélec, and C. Grouhel, 1998: Ozone climatologies at 9–12 km altitude as seen by the MOZAIC airborne program between September 1994 and August 1996. *J. Geophys. Res.,* **103,** 25 653–25 679.

Udelhofen, P. M., and D. L. Hartmann, 1995: Influence of tropical cloud systems on the relative humidity in the upper troposphere. *J. Geophys. Res.,* **100,** 7423–7440.

Waliser, D. E., and C. Gautier, 1993: A satellite-derived climatology of the ITCZ. *J. Climate,* **6,** 2162–2174.

Wang, J., D. J. Carlson, D. B. Parsons, T. F. Hock, D. Lauritsen, H. L. Cole, K. Beierle, and E. Chamberlain, 2003: Performance of operational radiosonde humidity sensors in direct comparison with a chilled mirror dew-point hygrometer and its climate implication. *Geophys. Res. Lett.,* **30,** 1860, doi:10.1029/2003GL016985.

Wu, X., J. J. Bates, and S. J. S. Khalsa, 1993: A climatology of the water vapor band brightness temperature from NOAA operational satellites. *J. Climate,* **6,** 1282–1300.

Yulaeva, E., and J. M. Wallace, 1994: The signature of ENSO in global temperature and precipitation fields derived from the microwave sounding unit. *J. Climate,* **7,** 1719–1736.

Zhang, C., B. E. Mapes, and B. J. Soden, 2003: Bimodality in tropical water vapour. *Quart. J. Roy. Meteor. Soc.,* **129,** 2847–2866.